JPP Journal of Pharmacy and Pharmacology
ROYAL PHARMACEUTICAL SOCIETY

JPP Journal of Pharmacy and Pharmacology

JPP 2011, 63: 1548–1558

Received January 31, 2011
Accepted August 29, 2011
DOI
10.1111/j.2042-7158.2011.01362.x
ISSN 0022-3573

Research Paper

An investigation on the correlation between drug dissolution properties and the growth behaviour of granules in high shear mixer

Zhen Guo[a], Mingxin Ma[b], Yanru Hao[c], Tongying Jiang[a] and Siling Wang[a]

[a]School of Pharmacy, Shenyang Pharmaceutical University, [b]Liaoning Institute for Food and Drug Control and [c]Shenyang B. Braun Pharmaceutical Co. Ltd, Shenyang, China

Abstract

Objectives The aim of this study was to investigate the correlation between the growth behaviour and in-vitro dissolution rate of water-insoluble drugs prepared with high-shear wet granulation.

Methods Granules containing nimodipine, microcrystalline cellulose, low-substituted hydroxypropylcellulose and aqueous solution of hydroxypropylcellulose were prepared and the effects of independent process variables, including impeller speed and liquid-to-solid ratio were taken into consideration. The mean granule size, granule-size distribution (GSD), porosity and surface properties were monitored at different kneading times to identify the granule-growth mechanisms simultaneously. A computer-based method was applied to simulate the dissolution behaviour of polydisperse granules based on the GSD data.

Key findings The in-vitro dissolution rate of drug was high for the early stages of granulation and sharply decreased when coalescence and consolidation of granules started, approaching a flat and low level when granules were sufficiently consolidated. The simulated dissolution results were in agreement with experimental observations and were significantly affected by the GSD, porosity and surface properties of granules during the granulation process. Moreover the GSD was directly related to the granule-growth behaviour and mechanisms.

Conclusions In general, it was concluded that the dissolution properties of nimodipine basically correlated with the growth behaviour of granules in a high-shear mixer. The simulation method based on GSD can be used as a convenient and rapid way to predict the dissolution properties for formulation development and granulation optimization.

Keywords computer simulation; granule growth behaviour; granule size distribution; high-shear granulation; in-vitro dissolution rate; nimodipine

Introduction

High-shear granulation has been widely used in the pharmaceutical industry and has many advantages over other techniques.[1,2] A great many papers focusing on the effect of the process parameters on granule properties have been published. The most investigated effects are the mixer load, impeller speed, mixing time,[3–5] temperature of the heating jacket,[6,7] chopper action,[4,7] binder content,[3,4] binder viscosity[8,9] and physical properties of the materials.[10,11] The mechanism of granule growth is another important research field. It has been reported that granule growth starts with the formation of large nuclei and proceeds continuously by the formation of small nuclei due to the repeated breaking and coalescence of the granules.[12,13] Efforts have also been directed at producing regime maps that describe and enable prediction of granule growth in high-shear mixers.[1,14] According to these studies, granules exhibit different physical properties at each stage of granule growth, including granule size distribution (GSD), specific area and granule porosities. However, it is important to investigate not only the granule properties but the dissolution properties of a drug product. There is little literature on the investigation of the relationship between granule-growth behaviour and drug dissolution properties.

Today, more than one-third of all new chemical entities suffer from poor aqueous solubility. For a drug of low aqueous solubility, particle size and resulting surface area may

Correspondence: Siling Wang, School of Pharmacy, No.32 P.O. Box, Shenyang Pharmaceutical University, No.103 Wenhua Road, Shenyang 110016, China. E-mail address: silingwang@syphu.edu.cn

have a significant effect on the rate of dissolution over the time interval during which gastrointestinal absorption occurs.[15] Several empirical and semi-empirical models have been presented to predict the dissolution rate from tablets and granules. These model-dependent methods involve curve-fitting of functions such as zero-order or first-order kinetics, Weibull and other models.[16,17]

Nimodipine (NMD) is classified in Class II in the Biopharmaceutics Classification Systems (BCS); this means that NMD has very low water solubility and high permeability. The dissolution rate is thus the absorption-rate-limiting factor.[18] The enhancement of dissolution rate is therefore a vital aspect in formulation development and granulation optimization.

In this paper, NMD was chosen as a model drug and the effects of the process parameters on growth behaviour and granule properties during a high-shear wet granulation process were evaluated. Moreover, a modified mixing-tank model[16] was used to simulate the dissolution rate of the drug in order to explore the correlation between the granule-growth behaviour and dissolution properties in the high-shear granulation process and develop a new, convenient and rapid way to predict the dissolution properties for formulation development and granulation optimization.

Materials and Methods

Materials

NMD (Shanxi Yabao Pharmaceutical Co. Ltd, China) was used as a model drug. Its solubility was 0.036 mg/100 ml in water.[18] The excipients used were microcrystalline cellulose (MCC Avicel® PH101, FMC Corporation, USA) as diluent, with a bulk density of 320 kg/m^3, a particle density of 1611 kg/m^3 and a mean particle size d_{50} of 50 μm, low-substituted hydroxypropylcellulose (L-HPC® (LH31)), Shin-Etsu Chemical Co. Ltd, Japan) as a disintegrant and 5% (w/w) aqueous solution of hydroxypropylcellulose (HPC-L®, Nippon Soda Co. Ltd, Japan) as liquid binder with a viscosity of 0.062 Pa s at 25°C All other materials were of analytical reagent grade.

Preparation of granules

Granules were produced in a laboratory-scale high-shear mixer (MicroGral®, Collette-NV, Belgium) equipped with a transparent 1-l glass vessel having an internal diameter of 126 mm and vertical side of height 120 mm, fitted with an impeller with three stainless steel blades of length 60 mm and a chopper with two stainless steel blades of length 15 mm, both of which rotated about a vertical axis (Figure 1). Granules were prepared with the same composition, containing 10% NMD, 85% MCC, 5% L-HPC and aqueous solution of 5% HPC-L (w/w). A batch of 100 g of the powders was loaded into the bowl and premixed for 2 min with an impeller speed of 200 rpm and a chopper speed of 1000 rpm before the binder was added. Granulation was then started by the addition of binder, which was poured at the middle point between the centre and the tip of the impeller with the impeller speed listed in Table 1. The chopper speed was four times faster than the impeller speed in order to maintain the same tip velocity.

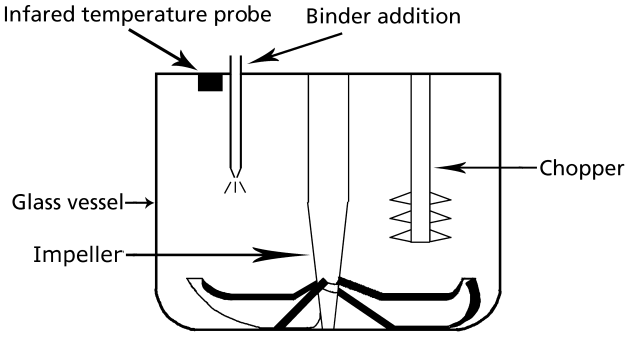

Figure 1 Schematic representation of the high-shear mixer.

Table 1 Operating conditions employed in this study ($n = 3$)

Run order	Trial number	Process parameters	
		Impeller speed (rpm)	L/S ratio (w/w)
3	1	300	0.700
7	2	300	0.750
5	3	300	0.800
9	4	500	0.700
1	5	500	0.750
6	6	500	0.800
4	7	700	0.700
2	8	700	0.750
8	9	700	0.800

A stopwatch was started immediately after addition of the binder and the kneading time in this work was considered to be the time taken to add all the binder. A new batch of powder and binder was used to produce a number of samples at each kneading time, the time ranging from 30 to 1500 s. Eleven batches were prepared and the batches stopped at 30, 60, 120, 180, 240, 300, 420, 600, 900, 1200 and 1500 s after binder addition. After production, granules were dried on a tray at 40°C for 24 h and stored in closed containers until their evaluation. Each experiment was performed in triplicate.

Experimental design

A two-factor, three-level face-centered central composite design was applied to describe the effects of process variables on the product characteristics.[19] Granules were produced with different settings of the process variables, as listed in Table 1. The trials were carried out in triplicate in a randomized order.

Granule characterization

Granule size distribution and specific surface area

The size analysis of granules was carried out with a vibrating apparatus (8411 Electric shaker, Hangzhou, China) using a set of nine standard sieves (76, 125, 200, 300, 450, 600, 800, 1250, 2000 μm). The sample size was 100 g and shaking was carried out for 10 min. The granule-size distribution was calculated from the ratio of the residual weight of the granules on each sieve to the granule weight before sieving. The surface area per unit volume is called the volume-specific surface (S_v).

In sieving analysis, S_v and the mean diameter (d_{sv}) can be obtained from the following equations:[20]

$$d_{sv} = \frac{\alpha_{sv}}{S_v} \quad (1)$$

$$S_v = \alpha_{sv} \sum \frac{W_r}{d_{a,r}} \quad (2)$$

where W_r is the fractional weight residing between two sieves of average aperture $d_{a,r}$ and α_{sv} is the surface-volume shape coefficient. In this article, a surface-volume shape coefficient $\alpha_{sv} = 6$ was selected.[21] This value was used for the calculation of the mean granule size (d_{sv}) and volume-specific surface (S_v) according to eqs (1) and (2).

Porosity measurement of granules

A technique of kerosene (analytical reagent grade, Tianjin, China) displacement was chosen to evaluate granule porosities. The porosity was measured by the pycnometric method as described previously.[22,23] The intra-granular porosity, ε, was calculated by the formula:

$$\varepsilon = 1 - \left(\frac{V_s}{V_g} \right) \quad (3)$$

where V_s is the volume of the solid particles and V_g is the volume of the granule.

For a granule prepared with a liquid/solid (L/S) ratio of β eq. 3 then becomes:

$$\varepsilon = 1 - \frac{\beta}{1+\beta} \cdot \frac{m_g / \rho_s}{V_g} = 1 - \frac{\beta}{1+\beta} \cdot \frac{\rho_g}{\rho_s} \quad (4)$$

where m_g is the mass of the granule, ρ_g is the density of the granule and ρ_s is the solid density of the mixed powder.

Scanning electron microscopy

The surface morphology of granules was observed by scanning electron microscopy (JSM-7001F, JEOL Ltd, Japan). Granules were mounted on a plate using carbon paint and coated with gold before examination.

Surface analysis by nitrogen adsorption

The surface and pore properties of the granules were analysed by the nitrogen adsorption method (SA3100 Surface Analyzer, Beckman Coult™, USA). The samples were outgassed at 60°C overnight under vacuum and nitrogen adsorption isotherms were measured at −196°C over an interval of relative pressures from 10^{-6} to 0.995 using nitrogen at 99.998% purity. The Brunauer–Emmett–Teller (BET) surface area was then calculated.

Solubility determination

The solubility of nimodipine was determined by equilibrating excess drug and an acetate buffer containing 0.3% of SDS (pH 4.5) with agitation at 37°C for two days in a thermostatically controlled water bath. After the equilibration period, aliquots were passed through a 0.22-μm millipore membrane filter. Samples were diluted and assayed by the UV-vis spectroscopy (UV-2000, Unico, China) method at 237 nm.[24] The solubility was determined to be 149 ± 1 μg/ml.

In-vitro dissolution test

A dissolution test of NMD from granules was conducted using a dissolution tester (RC-8D, Tianjin, China) in compliance with method II (paddle method) in ChP 2005 edition.[25] The dissolution medium used was 900 ml of acetate buffers containing 0.3% SDS (pH 4.5). Other parameters included paddle speed of 75 rpm and temperature of 37 ± 0.5°C. Granules equivalent to 30 mg NMD were added directly into the dissolution medium. Samples were taken at 5, 10, 15, 20, 30 and 45 min, and replaced with an equal volume of the same medium. An aliquot of 5 ml was filtered through a 0.22 μm filter. The sample solutions were diluted and the concentration of dissolved NMD was determined using the UV-vis method at 237 nm. In this study, the dissolution percentage after 30 min (hereafter 'D30') was used to evaluate the dissolution properties of granules according to ChP 2005 edition. All experiments were performed in triplicate.

Simulation of dissolution rate

An equation based on the Nernst–Brunner and Levich modifications of the Noyes–Whitney model can be used to describe the dissolution of monodisperse powders:[26]

$$\frac{dX_s}{dt} = \frac{DS}{h}\left(C_s - \frac{X_d}{V} \right) \quad (5)$$

where X_s is the mass of solid drug at any time, D is the drug diffusivity, S is the surface area, C_s is the aqueous solubility of the drug, h is the diffusion layer thickness, X_d is the mass of dissolved drug at any time and V is the volume of the dissolution medium. In this study, the dissolution rate was tested under sink conditions so that X_d/V could be neglected. The surface area S of polydisperse granules was simulated by treating it as the sum of several monodisperse fractions and replaced by the results S_v obtained from eq. (2). Then eq. (5) could be modified as:

$$\frac{dX_s}{dt} = \frac{\alpha_{sv} D C_s}{h} \sum \frac{W_r}{d_{a,r}} \quad (6)$$

In order to simulate dissolution profiles from granule-size data, the diffusion layer thickness h was taken to be equal to the granule radius up to 30 μm, above which it was assumed to be constant at 30 μm.[15] The solubility of NMD C_s was determined in the above section and was found to be 149 ± 1 μm/ml while the diffusion coefficient was estimated using Nakanishi correlation:[27,28]

$$D_{AB} = \left[\frac{9.97 \times 10^{-8}}{(I_A V_A)^{1/3}} + \frac{2.40 \times 10^{-8} A_B S_B V_B}{I_A S_A V_A} \right] \frac{T}{\eta_B} \quad (7)$$

where $A_B = 2.8$, $S_B = 1$ for water and $I_A = S_A = 1$ for NMD, and the viscosity of the dissolution medium η_B at 37°C was determined to be 0.6989 mPa s using a rheometer (AR 2000ex, TA Instrument, USA). The molar volumes V_A and V_B for NMD and water were estimated using Schroeder's method.[29] Finally, the diffusion coefficient was calculated as 7.03×10^{-6} cm^3 s^{-1}.

Statistical analysis

The differences in the results of dissolution tests were evaluated using analysis of variance (ANOVA) with SPSS software (SPSS Inc., Chicago, USA) and $P \leq 0.05$ was considered statistically significant. All results presented are the mean of three determinations.[4]

Results

Effects of process parameters on granule growth

The effects of varying the L/S ratio on the mean granule size at an impeller speeds of 300, 500 and 700 rpm are shown in Figure 2. It can be seen that the ultimate mean granule size was determined by the amount of binder added, increasing in proportion to increases in L/S ratio, particularly at a high impeller speed. Moreover, the impeller speed significantly affected the granule growth rate. There were significant increases in the rate of granule growth rate at each L/S ratio with increasing impeller speed.

The process of granule growth can be described by Figure 3, which represents the evolution of GSD in experiments with limiting operating conditions.[30,31] Experiments with a low and medium impeller speed exhibited a 'peak' on the growth curve during the early stages of granule growth. The mean granule size slightly decreased right after the 'peak' and then increased steadily to the final granule size. However, this phenomenon was not present in the high impeller speed experiments (Trials 7, 8 and 9). Granules larger than 1250 μm were manufactured in each experiment during the early stages, especially in the experiments with high binder content. When the impeller speed was high enough, the large weak granules could not resist the high shear strength and fragmented immediately after formation (Figure 3D: lines a and b) in contrast with the experiment at a low shear rate (Figure 3B: lines a to f). The same findings were also obtained from Figure 3A even though there were fewer coarse granules found in the early stages due to the low binder content. In contrast, owing to the high impeller speed and low binder content, there were few large granules produced in Figure 3C. The results obtained from the GSD analysis above imply that the early granules formed are weak and short-lived. Granules exhibit steady growth behaviour immediately after the fragmentation. The mean granule size increased steadily to a plateau, which was defined as the final granule size. The rate of granule growth increased in proportion to the impeller speed. The mean granule size generally levelled off after the steady increase, while an obvious decrease in mean granule size could be found in the curve of trials with a high impeller speed and low/medium binder content (Figure 2c).

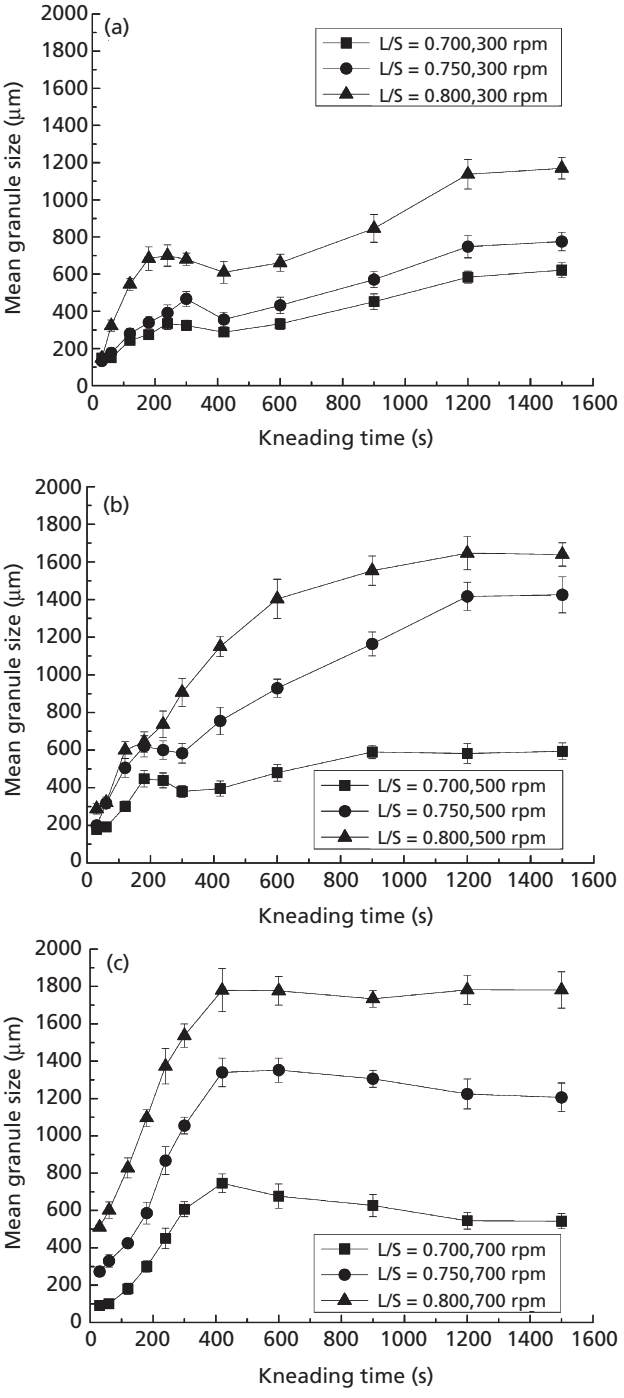

Figure 2 Comparisons of mean granule size under the same impeller speed: (A) 300 rpm, (B) 500 rpm and (C) 700 rpm.

Dissolution rate with different process parameters

An in-vitro dissolution test of NMD from granules manufactured under various operating conditions was conducted. Figure 4 shows the dissolution profile for Trial 1, which demonstrates that the dissolution of NMD from granules

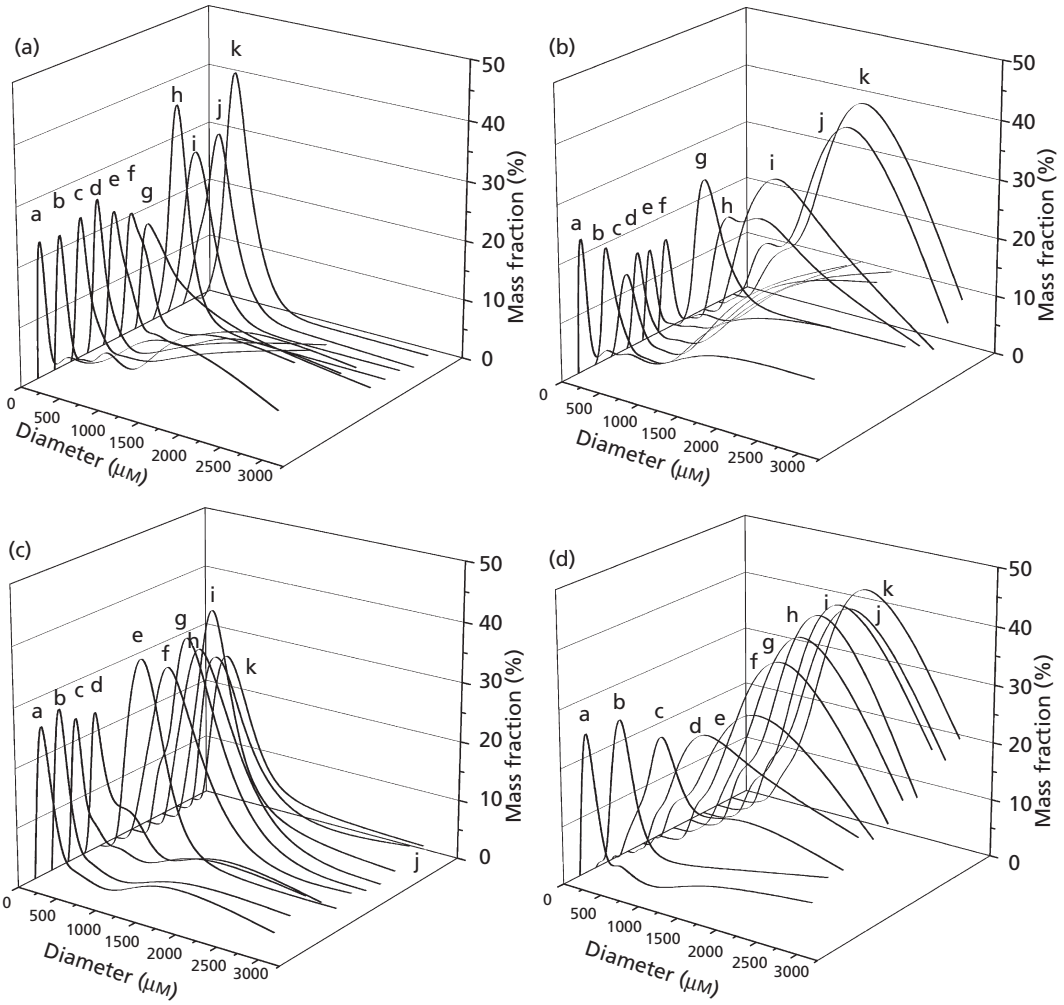

Figure 3 Change of GSD during granulation process with limiting operating conditions: (A) L/S = 0.700, 300 rpm, (B) L/S = 0.800, 300 rpm, (C) L/S = 0.700, 700 rpm and (D) L/S = 0.800, 700 rpm.

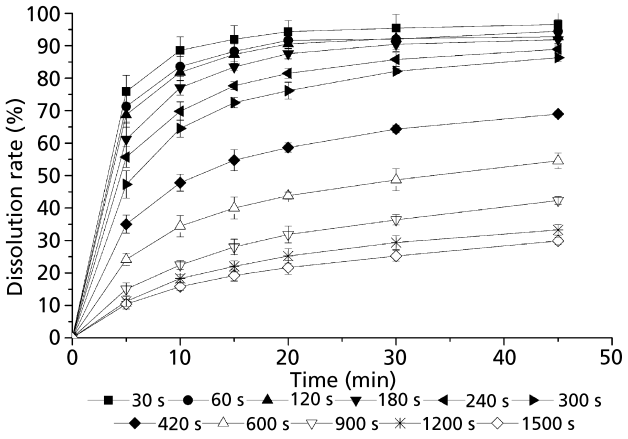

Figure 4 Dissolution profiles for granules prepared in Trial 1 at different kneading times.

decreased with granulation processing. Trials 2–9 exhibited similar dissolution properties (not shown).

The dissolution percentage after 30 min was used as a criterion to evaluate the quality of tablets and capsules in accordance with the ChP 2005 edition. Figure 5 illustrates the effects of the process parameters on the dissolution rate of NMD after 30 min and Table 2 shows the ANOVA results. It can be determined that granules manufactured with same impeller speed displayed similar dissolution properties (Figure 5(d)–(f); $P \geq 0.05$) in contrast to the granules with the same L/S ratio, which displayed different dissolution properties (Figure 5(a)–(c); $P \leq 0.05$). In other words, the effect of binder amount added was less than that of the impeller speed.

The simulation study, as shown by the dashed curves in Figure 5, was conducted using a computer program based on the sieving data obtained from Trials 1–9. The results demonstrate that the supposed model and parameters accurately reflect the dissolution properties of NMD granules.

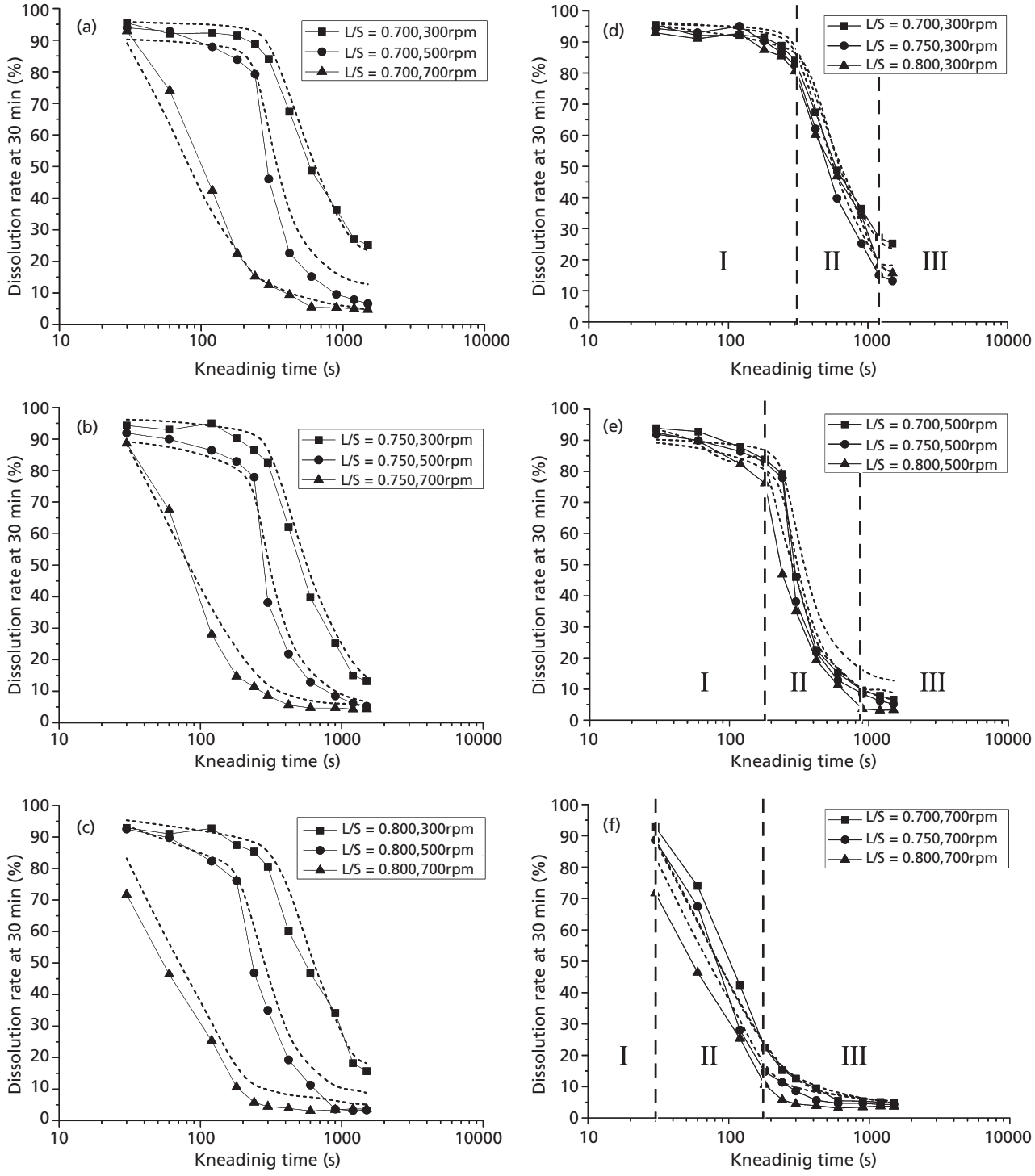

Figure 5 D30 of NMD granules sorted by L/S ratio: (A) 0.700, (B) 0.750, (C) 0.800; and sorted by impeller speed: (D) 300 rpm, (E) 500 rpm, (F) 700 rpm. Dashed lines represent the simulated dissolution profiles based on the GSD. D30 curves can be divided into three phases: (I) a slight decreasing phase, (II) a sharp collapse phase and (III) a steady phase.

Results of granule porosity

The porosities of the granules for each trial were calculated using eqs (3) and (4) and the results are shown in Figure 6 as a function of the kneading time categorized by different operating parameters. The data indicate that the porosity exhibited a decreased tendency during granulation processing. Figure 6 also shows the effects of process parameters on granule porosity. Granules agglomerated with a high impeller speed were consolidated by further impact strength and therefore the general porosity of granules was in inverse proportion to the

Table 2 Analysis of variance of the D30 results under different operating conditions

Process parameter	Statistical parameters	Sorted by L/S ratio					
		L/S = 0.700		L/S = 0.750		L/S = 0.800	
		Between groups	Within groups	Between groups	Within groups	Between groups	Within groups
Impeller speed	Sum of squares	0.9622	3.1851	0.9383	0.3352	1.4875	2.2845
	Mean square	0.4811	0.1062	0.4692	0.1112	0.7438	0.0762
	F value	4.531		4.220		9.767	
	Significance (*P*)	0.019		0.024		0.001	
Process parameters being studied	**Statistical parameters**	**Sorted by impeller speed**					
		IS = 300 rpm		IS = 500 rpm		IS = 700 rpm	
		Between groups	Within groups	Between groups	Within groups	Between groups	Within groups
L/S ratio	Sum of squares	0.0141	2.8669	0.0324	4.2520	0.0525	2.2904
	Mean square	0.0070	0.0956	0.0162	0.1417	0.0262	0.0764
	F value	0.073		0.114		0.344	
	Significance (*P*)	0.929		0.892		0.712	

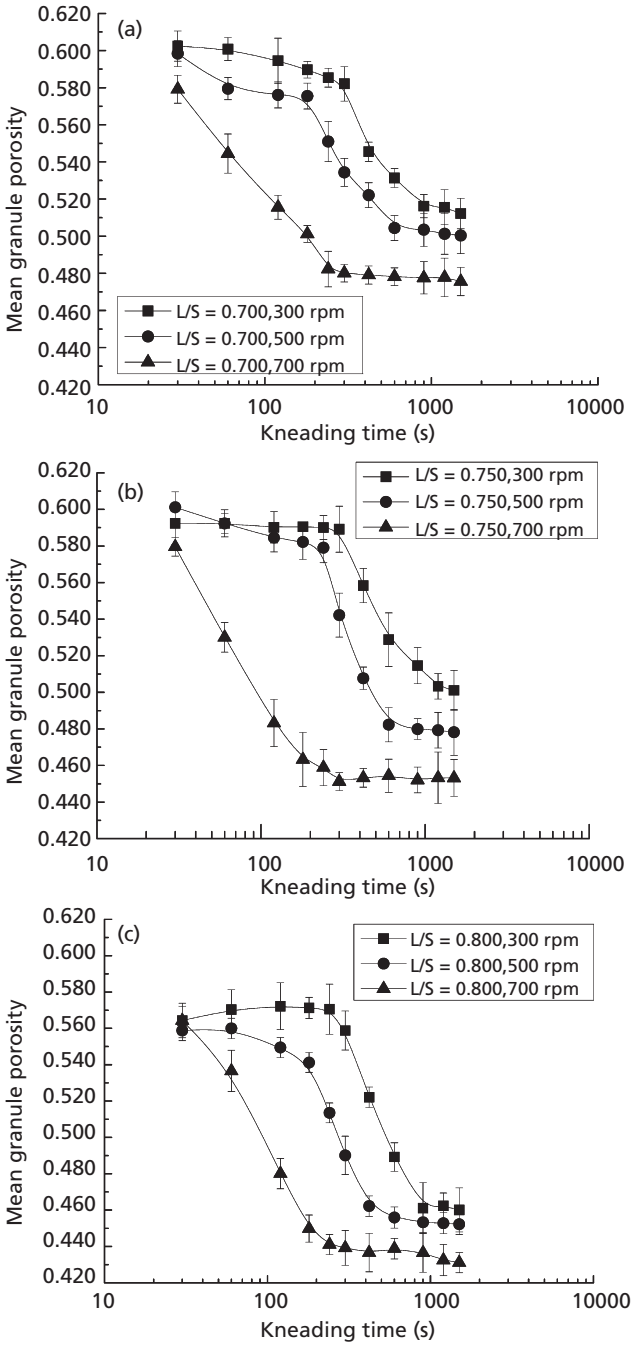

Figure 6 Comparisons of granule porosities under the same L/S ratio: (a) L/S = 0.700, (b) L/S = 0.750, (c) L/S = 0.800.

impeller speed.[32] Moreover, granule porosity decreased with binder content because more binder led to larger and more compact granules, in accordance with the results from Figure 2 and the previous studies.[33,34]

Results of granule surface property analysis

Brunauer–Emmett–Teller surface area analysis results

Figure 7 depicts the BET surface area of granules manufactured with different impeller speeds, L/S ratios and kneading

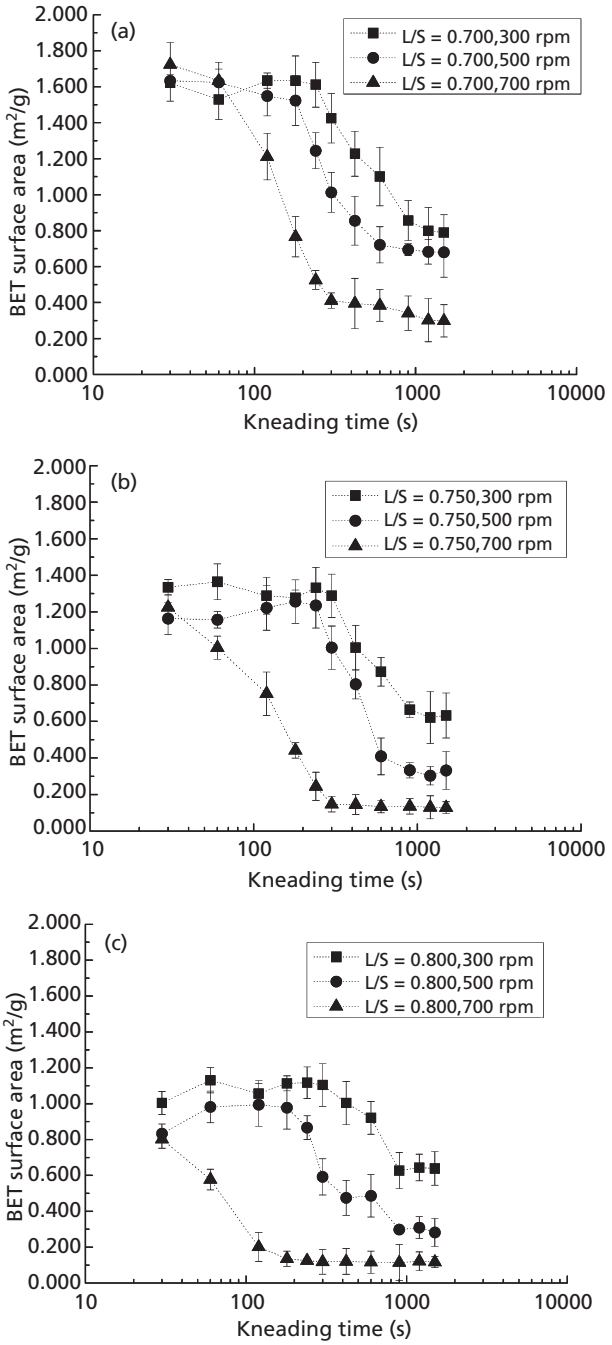

Figure 7 BET surface area values of granules under different process variables: (a) L/S = 0.700, (b) L/S = 0.750, (c) L/S = 0.800.

times. Similar to the results of the granule porosity analysis, the general surface values are also inversely proportional to the impeller speed and L/S ratio.

Scanning electron microscopy results

Figure 8 shows the scanning electron microphotographs of the granules prepared under different operating conditions. The surface morphology photos show that granules were consolidated during the growing process.[35] The kneading time significantly affected the surface morphology of the granules. Figure 8(a), (d) and (g) show the surface images of granules during early stages of granulation. It can be seen that the surface of the granules is extremely rough, which suggests that there are a great many irregular powder particles on the granule surfaces. The granules become smooth and uniform as granulation proceeds because of granule/granule and granule/wall collisions due to the impeller and chopper.[30]

From the comparison of photos of granules with the same kneading time, it can be seen that the impeller speed also greatly affects the surface morphology. A high impeller speed promotes the consolidation of granules and decreases the surface area, a finding that is shown in Figure 7. On the other hand, similar surface images are observed in Figure 8(j)–(l) and (m)–(o) where L/S ratio is increased at the same impeller speed and kneading time. The effect of binder content on the surface properties is therefore less than that of impeller speed.

Discussion

Granule growth mechanisms

A schematic diagram of granule growth mechanism, as summarized by Vonk *et al.*,[12] is shown in Figure 9. At the moment the droplet of binder reaches the moving powder bed, a loose primary nucleus forms due to layering, which can be characterized by a high porosity and low tensile strength (Figure 8(a), (d) and (e)). The primary nuclei then break into fragments because of the action of the impeller and chopper. The break-up of primary nuclei produces many small secondary nuclei, which are the starting materials for the coalescence. The coalescence starts when the solid mass is sufficiently wetted and densification of the secondary nuclei occurs (Figure 8(b) and (e)). As the coalescence proceeds, the growth rate decreases gradually because no more binder is applied. Finally, the growth and breakage of granules reaches an equilibrium state and the granule size remains constant (Figure 8(f) and (i)).

Correlation between dissolution properties and granule growth behaviour

In this study, the surface area that was used to simulate the dissolution rate of granules was estimated by the GSD although other methods such as gas adsorption were more accurate. GSD is widely used and more convenient and rapid than any other method during industrial practice.[36] Comparing Figures 5 and 7, it was observed that the results of BET surface area had the same properties as the results of simulated dissolution curves; this proved that the estimated volume-specific surface (S_v) was apposite to simulate the granule dissolution rate.

Previous studies have suggested that the dissolution rate of drug crystals is significantly affected by particle size and could be simulated theoretically under non-sink conditions.[15,28] The particle size directly determines the contact area between the drug and the dissolution medium, which is the key factor for drug dissolution. According to eq. (2), surface area depends on the GSD of granules and increases when the mass fraction of small-size granules increases. For high-shear granulation, the GSD is critically related to the

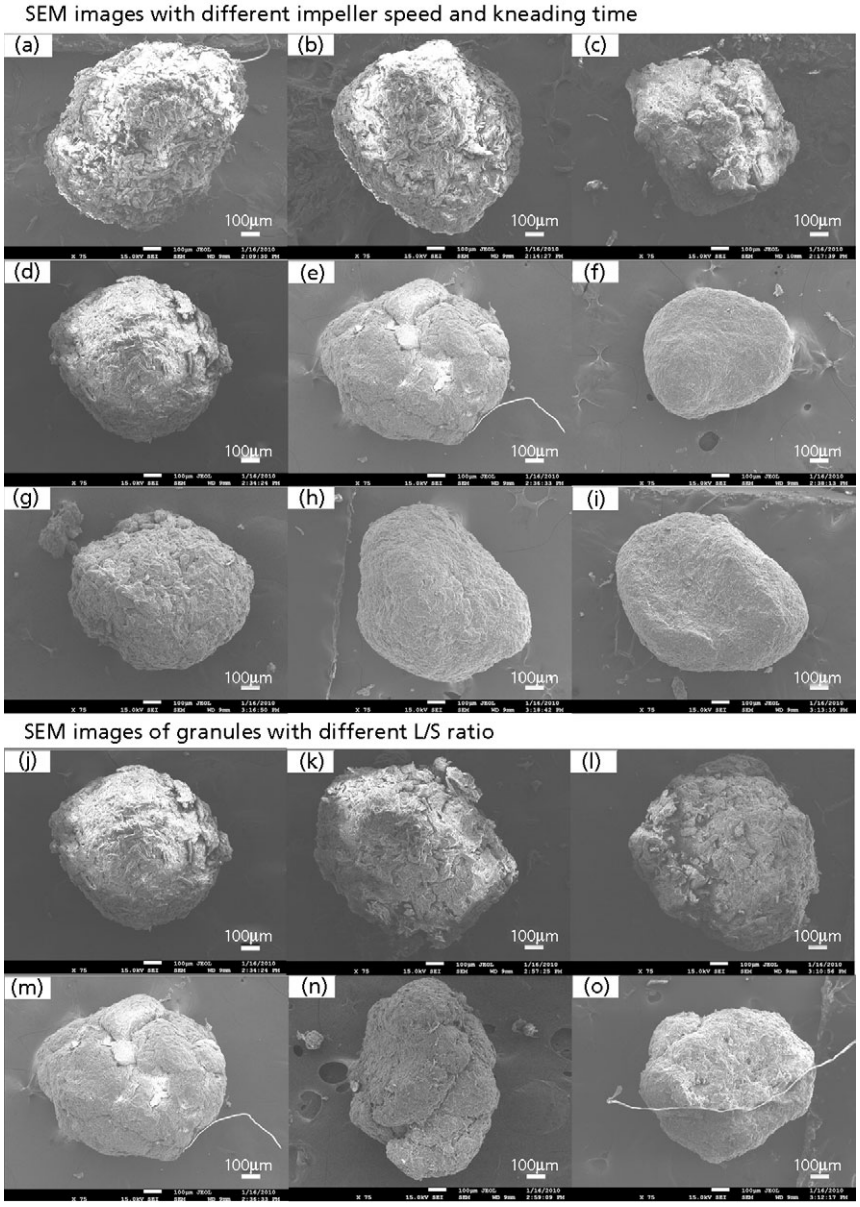

Figure 8 Scanning electron microscope images of granules obtained under different operating conditions: IS = 300 rpm, L/S = 0.700 with kneading time: (A) 180 s, (B) 600 s, (C) 1500 s; IS = 500 rpm, L/S = 0.700 with kneading time: (D) 180 s, (E) 600 s, (F) 1500 s; IS = 700 rpm, L/S = 0.700 with kneading time: (G) 180 s, (H) 600 s, (I) 1500 s; IS = 500 rpm, kneading time = 180 s with L/S ratio: (J) 0.700, (K) 0.750, (L) 0.800; IS = 500 rpm, kneading time = 600 s with L/S ratio: (M) 0.700, (N) 0.750, (O) 0.800.

granule growth behaviour. The dissolution curves in Figure 5 can be divided into three phases: (1) a slightly decreasing phase where the dissolution rate decreases less than 20% during the early granulation stage and which is identified as the nucleation and fragmentation mechanism according to the analysis of growth behaviour; (2) a sharp collapse phase, where the dissolution rate of the drug sharply collapses to less than 20% of total drug content, when coalescence and consolidation progress; (3) a steady phase where the dissolution rate approaches a flat and low level, and in which granules are sufficiently consolidated by the impeller/granule, granule/granule and granule/wall collisions.

A schematic diagram summarizing the correlation between dissolution properties and granule growth behaviour is shown in Figure 10. The dissolution rate of the granules depends on granule properties such as size, porosity and surface area. Since it has already been shown that the mechanical properties of granules are influenced by the growth behaviour during granulation, it would be sensible to expect that the granule growth behaviour significantly affects the drug dissolution rate. The high dissolution rate of granules kneaded for short times (before the turning point) may be explained by the larger surface area and consequent larger contact area between drug and dissolution medium. As the granulation

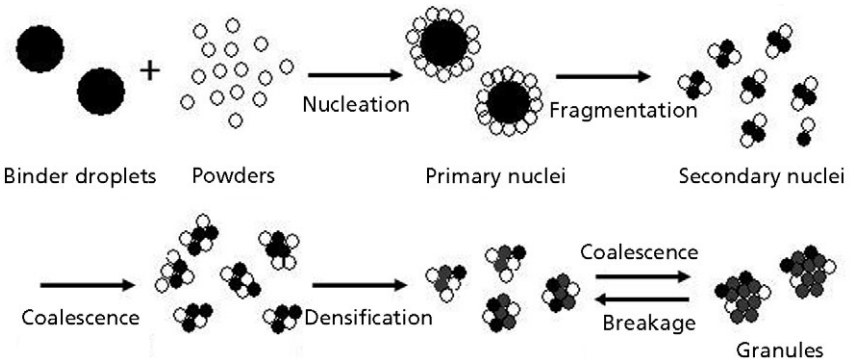

Figure 9 Growth mechanisms of granules in high-shear mixer.[12]

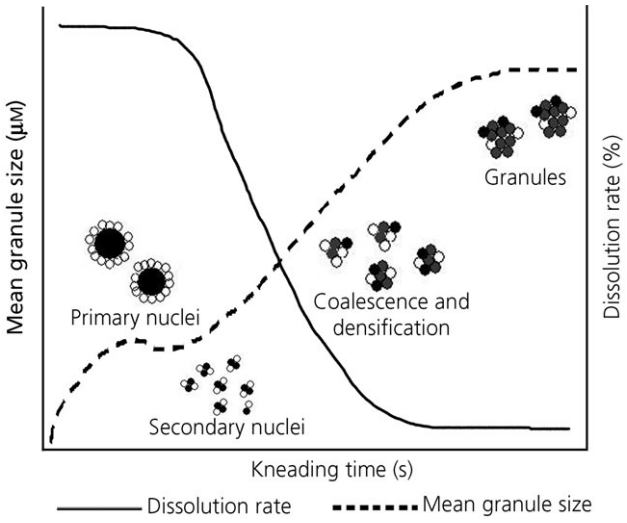

Figure 10 Schematic diagram outlining the relationship between drug dissolution rate and granule growth.

process progresses, coalescence mechanisms become dominant and secondary nuclei collide with each other while granule size dramatically increases.[37] Therefore, the surface area sharply decreases with coalescence and consolidation of granules, leading to the prevention of drug release. Finally, the dissolution rate levels off when granules are well agglomerated and the final dissolution rate is determined by the porosity, which is affected by the L/S ratio. To sum up, the dissolution rate of NMD basically correlates with the growth behaviour of granules in a high-shear mixer.

Conclusions

In the present study, the overall effects of impeller speed and L/S ratio on granulation behaviour in a high-shear mixer were investigated and the different phases of granule growth were also identified by monitoring the GSD, porosity, surface morphology and surface area. The results revealed that granules exhibit different surface properties according to the different growth mechanisms, which can be controlled by the operating conditions.

The drug dissolution rate is high during the early stages of granulation and sharply decreases when coalescence and consolidation of granules starts. The simulated dissolution results were in agreement with experimental observations and are significantly affected by the GSD during granulation process.

In general, it was concluded that the dissolution properties of NMD basically correlate with the growth behaviour of granules in a high-shear mixer. The simulation method based on GSD can be used as a convenient and rapid way to predict the dissolution properties for formulation development and granulation optimization.

Declarations

Conflict of interest

The Author(s) declare(s) that they have no conflicts of interest to disclose.

Funding

This work was supported by the National Basic Research Program of China (973 Program) (No. 2009CB930300) and the Major National Platform for Innovative Pharmaceuticals (No. 2009ZX09301-012). The authors would like to thank Collette N.V., Belgium, for supplying the MicroGral® high-shear mixers and for their logistic and technical support.

References

1. Iveson SM *et al*. Growth regime map for liquid-bound granules: further development and experimental validation. *Powder Technol* 2001; 117: 83–97.
2. Parikh DM. *Handbook of Pharmaceutical Granulation Technology*, 2nd edn. New York: Taylor & Francis Group, 2005.
3. Schaefer T *et al*. Melt pelletization in a high shear mixer. I. Effects of process variables and binder. *Acta Pharm Nord* 1992; 4: 133–140.
4. Wang S *et al*. Investigation of high shear wet granulation processes using different parameters and formulation. *Chem Pharm Bull* 2008; 56: 22–27.
5. Heng PWS *et al*. Effects of process variables and their interactions on melt pelletization in a high shear mixer. *STP Pharma Sci* 2000; 10: 165–172.
6. Schaefer T *et al*. Melt pelletization in a high shear mixer. VI. Agglomeration of cohesive powder. *Int J Pharm* 1996; 132: 221–230.
7. Voinovich D *et al*. Screening of high shear mixer melt granulation process variables using an asymmetrical factorial design. *Int J Pharm* 1999; 190: 73–81.

8. Keningley ST *et al*. An investigation into the effects of binder viscosity on agglomeration behaviour. *Powder Technol* 1997; 91: 95–103.
9. Mills PTJ *et al*. The effect of binder viscosity on particle agglomeration in a low shear mixer/agglomerator. *Powder Technol* 2000; 113: 140–147.
10. Schaefer T *et al*. Melt pelletization in a high shear mixer. III. Effects of lactose quality. *Acta Pharm Nord* 1992; 4: 245–252.
11. Realpe A, Velázquez C. Growth kinetics and mechanisms of wet granulation in a laboratory-scale high shear mixer: effect of initial polydispersity of particle size. *Chem Eng Sci* 2008; 62: 1602–1611.
12. Vonk P *et al*. Growth mechanisms of high-shear pelletization. *Int J Pharm* 1997; 157: 93–102.
13. Knight PC *et al*. An investigation into the kinetics of liquid distribution and growth in high shear mixer agglomeration. *Powder Technol* 1998; 97: 246–257.
14. Iveson SM, Litster JD. Growth regime map for liquid-bounded granules. *AIChE J* 1998; 44: 1510–1518.
15. Hintz RJ, Johnson KC. The effect of particle size distribution on dissolution rate and oral absorption. *Int J Pharm* 1989; 51: 9–17.
16. Dressman JB, Fleisher D. Mixing-tank model for predicting dissolution rate control of oral absorption. *J Pharm Sci* 1986; 75: 109–116.
17. Sathe PM *et al*. In-vitro dissolution profile comparison: statistics and analysis, model dependent approach. *Pharm Res* 1996; 13: 1799–1803.
18. Grunenberg A *et al*. Polymorphism in binary mixtures, as exemplified by nimodipine. *Int J Pharm* 1995; 118: 11–21.
19. Dévay A *et al*. Investigation on drug dissolution and particle characteristics of pellets related to manufacturing process variables of high-shear granulation. *J Biochem Biophys Methods* 2006; 69: 197–205.
20. Wang Q *et al*. Dissolution kinetics of guar gum powders-III. Effect of particle size. *Carbohydr Polym* 2006; 64: 239–246.
21. Allen T. *Powder Sampling and Particle Size Determination*, 1st edn. Amsterdam: Elsevier Science, 2003.
22. Iveson SM *et al*. Fundamental studies of granule consolidation part 1: effects of binder content and binder viscosity. *Powder Technol* 1996; 88: 15–20.
23. Rough SL *et al*. A regime map for stages in high shear mixer agglomeration using ultra-high viscosity binders. *Adv Powder Technol* 2005; 16: 373–386.
24. He Z *et al*. Development of a dissolution medium for nimodipine tablets based on bioavailability evaluation. *Eur J Pharm Sci* 2004; 21: 487–491.
25. *Chinese Pharmacopoeia*, 2005 edn. Beijing: Chemical Industry Press, 2005.
26. Dressman JB *et al*. Dissolution testing as a prognostic tool for oral drug absorption: immediate release dosage forms. *Pharm Res* 1998; 15: 11–22.
27. Cantrel L *et al*. Diffusion coefficients of molecular iodine in aqueous solutions. *J Chem Eng Data* 1997; 42: 216–220.
28. Xia D *et al*. Effect of crystal size on the in vitro dissolution and oral absorption of nitrendipine in rats. *Pharm Res* 2010; 27: 1965–1976.
29. Poling BE *et al*. *Properties of Gases and Liquids*, 5th edn. New York: McGraw-Hill, 2000.
30. Tu W *et al*. Exploring the regime map for high-shear mixer granulation. *Chem Eng J* 2009; 145: 505–513.
31. Benali M *et al*. Effect of operating conditions and physic-chemical properties on the wet granulation kinetics in high shear mixer. *Powder Technol* 2009; 190: 160–169.
32. Mangwandi C *et al*. Effect of impeller speed on mechanical and dissolution properties of high-shear granules. *Chem Eng J* 2010; 164: 305–315.
33. Schaefer T *et al*. Melt granulation in a laboratory scale high shear mixer. *Drug Dev Ind Pharm* 1990; 16: 1249–1277.
34. Ramachandran R *et al*. Experimental studies on distributions of granule size, binder content and porosity in batch drum granulation: inferences on process modelling requirements and process sensitivities. *Powder Technol* 2008; 188: 89–101.
35. Ohno I *et al*. Importance of evaluating the consolidation of granules manufactured by high shear mixer. *Int J Pharm* 2007; 338: 79–86.
36. Lines RW. The work of the British standards institution in particle, surface and pore size characterisation. *Part Part Syst Charact* 1991; 8: 170–172.
37. Liu LX *et al*. Coalescence of deformable granules in wet granulation process. *AIChE J* 2000; 46: 529–539.